Infrared Spectroscopic Studies of Mono-, Di-, and Trihydrido C−H Insertion Complexes Formed in Reaction of Ethylene with Laser-Ablated Hafnium Atoms and Isolated in a Solid Argon Matrix

Han-Gook Cho and Lester Andrews*

Department of Chemistry, P.O. Box 400319, University of Virginia, Charlottesville, Virginia 22904-4319

Received: May 21, 2004; In Final Form: July 19, 2004

The C−H insertion reaction of laser-ablated Hf atoms with ethylene in excess argon has been carried out during codeposition at 7 K, and the reaction products have been investigated by means of infrared spectroscopy. Parallel to the case of Zr, mono-, di-, and trihydrido C−H insertion complexes are identified. Among them, the mono- and dihydrido C−H insertion complexes are reaction intermediates of hydrogen elimination from ethylene by second-row transition-metal atoms presumed in previous reaction dynamics studies. The higher Hf−H stretching frequencies and shorter Hf−H and C−Hf bond lengths of the hafnium C−H insertion products than those of the zirconium products are attributed to the shortened bonds of the heavier metal atom by relativistic effects.

Introduction

The C−H insertion reaction of ethylene by vaporized transition-metal atoms has recently drawn broad attention. Siegbahn, Blomberg, and Svensson theoretically investigated the activation of the C−H bond by second-row transition-metal atoms.[1−4] Their study showed that early transition-metal atoms first form a strongly bound complex with ethylene, which later rearranges to an insertion product. Later, Parnis et al. measured the reaction rate coefficients for several hydrocarbons including ethylene with early second-row transition metals and their neutral diatomic oxides.[5] They concluded that the C−H bond insertion step followed by the elimination of H_2 is indeed the operative mechanism for the reaction of both metal atoms and metal oxides.

Such C−H insertion of ethylene often leads to H_2 elimination. In a series of studies, Weisshaar and co-workers investigated the reactivity of ground-state, neutral, early second-row transition-metal atoms with alkenes.[6−10] Using a fast-flow reactor and 157-nm photoionization scheme, they identified $M-C_2H_2^+$, along with $M-C_2H_4^+$, and explained their results on the basis of the reaction mechanism following the reaction path[11]

$$\text{M} + \text{ethylene} \rightarrow \pi\text{-complex} \rightarrow \text{insertion product} \rightarrow \text{dihydrido complex} \rightarrow \text{M}-\text{C}_2\text{H}_2 + \text{H}_2$$

Initial formation of the weakly bound π-complex is presumably followed by transformation to a long-lived metallacyclopropane complex.[11−13] However, remaining parts of the reaction mechanism, particularly following the C−H insertion, hydrogen migration to the dihydrido complex, and the elimination of hydrogen, still need to be examined.

In a recent study, Lee et al. identified two C−H insertion products from the reaction of ethylene and Ti atoms on the basis of the differences in the relative increase in intensity upon electronic excitation of Ti with irradiation of visible light.[14] They assigned the two groups of absorption bands to the two oxidative reaction products, the insertion and a metallic cyclic dihydride species, the mono- and dihydrido Ti−ethylene complexes. More recently, the reaction of ethylene with laser-ablated Zr atoms has been investigated, and three C−H insertion products were identified (mono-, di-, and trihydrido Zr−ethylene complexes) on the basis of the behaviors of the product absorptions on photolysis and annealing.[15] Among them, the mono- and dihydrido complexes are the reaction intermediates presumed in earlier reaction dynamics studies of hydrogen elimination of ethylene by vaporized zirconium atoms.

It is therefore an intriguing question whether hafnium, the last naturally available group 4 transition metal, also forms similar C−H insertion products with ethylene. Hafnium also shows the interesting effects of decreasing atomic size owing to relativistic effects on the electrons[16−19] (i.e., shortening of bonds and high vibrational frequencies of the products[20−22]). In this study, the reaction of ethylene with laser-ablated hafnium atoms diluted in argon was carried out, and the products isolated in an argon matrix were identified by isotopic substitution and DFT calculations. Studies on reactions of the very high temperature metal hafnium with hydrocarbons are rare, and this is probably the first attempt at oxidative addition of hafnium atoms to the C−H bonds of a hydrocarbon.

Experimental and Computational Methods

Laser-ablated Hf atoms (Johnson−Matthey) were reacted with C_2H_4, C_2D_4, $^{13}C_2H_4$ (Cambridge Isotope Laboratories, 99%), and CH_2CD_2 (MSD Isotopes) in excess argon during condensation at 7 K using a closed-cycle He refrigerator (Air Products HC-2). The methods have been previously described in detail elsewhere.[23−26] Concentrations of the gas mixtures are typically 0.5% in argon. After reaction, infrared spectra were recorded at a resolution of 0.5 cm^{-1} using a Nicolet 550 spectrometer with a HgCdTe detector. Samples were later irradiated by a combination of optical filters and a mercury arc lamp (175 W) and subsequently annealed.

Complementary density functional theory (DFT) calculations were carried out using the *Gaussian 98* package,[27] B3LYP density functional, 6-311+G(2d,p) basis sets for C and H, and

* Author for correspondence. E-mail: lsa@virginia.edu.

10.1021/jp0477957 CCC: $27.50
Published on Web 10/28/2004

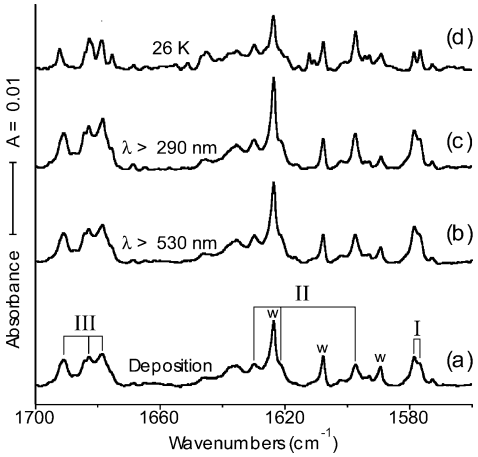

Figure 1. IR spectra in the region of 1560−1700 cm^{-1} for laser-ablated Hf atoms codeposited with Ar/C_2H_4 at 7 K. (a) Hf + 0.5% C_2H_4 in Ar codeposited for 1 h, (b) after broad-band photolysis with a filter (>530 nm) for 15 min, (c) after broad-band photolysis with a filter (>290 nm) for 15 min, and (d) after annealing to 26 K. I, II, or III stands for the group the product band belongs to. w indicates water impurity absorptions.

LanL2 pseudopotential and LanL2DZ basis set for Hf to provide a consistent set of vibrational frequencies for the reaction products. Geometries were fully relaxed during optimization, and the optimized geometry was confirmed via vibrational analysis. Calculations with the keyword STABLE ensured that the converged electronic state is the stable ground state. In calculation of the binding energy of a metal complex, the zero-point energy is included.

Results and Discussion

The spectral features in the Hf + ethylene spectrum are surprisingly similar to those in the Zr + ethylene spectrum.[15] Shown in Figure 1 is the IR spectrum in the region of 1560−1700 cm^{-1} for laser-ablated Hf atoms codeposited with Ar/C_2H_4 at 7 K and its variation upon photolysis and annealing. New product absorptions are observed at 1576.8, 1578.7, 1597.5, 1621.6, 1630.1, 1679, 1683, and 1691.2 cm^{-1}. The ^{13}C substitution leads to negligible shifts in frequencies of the absorptions, whereas deuteration results in large shifts in the frequencies, as shown in Figure 2, indicating that these absorptions all arise from the Hf−H stretching modes of the reaction products. In earlier studies, the hydrogen stretching absorptions of hafnium hydrides were observed in the same frequency region.[20,21]

The hydrogen stretching absorptions all grow on visible irradiation (λ > 530 nm), but the growth percentages are not the same. While the split absorptions at 1576.8 and 1578.7 cm^{-1} (marked with I) and the absorptions at 1679, 1683, and 1691.2 cm^{-1} (marked with III) increase about 20%, the absorptions at 1597.5, 1621.6, and 1630.1 cm^{-1} (marked with II) grow about 50%. Noticeable changes in the product absorptions are not observed on irradiation with other filters (λ > 460 nm, λ > 420 nm, λ > 380 nm, and λ > 320 nm); however, following irradiation with λ > 290 nm, the absorptions at 1597.5, 1621.6, and 1630.1 cm^{-1} (II) increase by 30%, and the absorptions at 1679, 1683, and 1691.2 cm^{-1} (III) grow another 15%, while the absorptions at 1576.8 and 1578.7 cm^{-1} (I) remain the same. Group II absorptions grow even further on annealing to 26 K, while groups I and III absorptions decrease. The spectral variations on photolysis and annealing are also very similar to those in the Zr + ethylene system.[15]

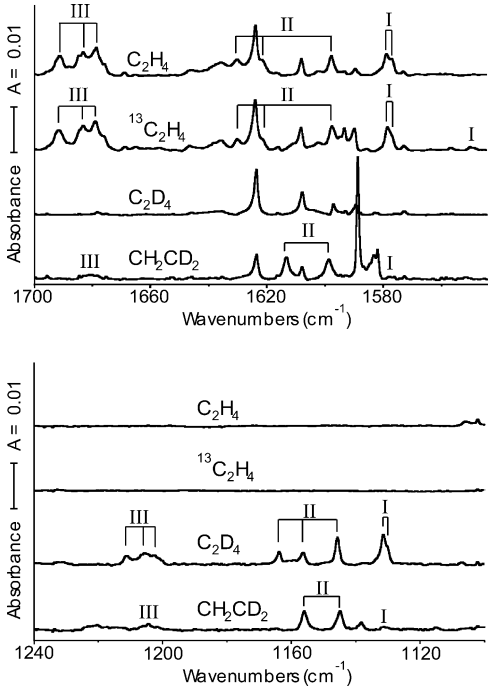

Figure 2. IR spectra in the regions of 1544−1700 and 1110−1240 cm^{-1} for laser-ablated Hf atoms codeposited with ethylene isotopomers diluted in Ar at 7 K. The product absorptions are identified with I, II, or III, depending on the absorption group.

TABLE 1: Frequencies of Observed Product Absorptions[a]

group	C_2H_4	C_2D_4	$^{13}C_2H_4$	CH_2CD_2
I	**1578.7**, 1576.9	**1131.6**, 1130.3	**1578.3**, 1576.6	1578.3
		1380.0, 1378.0	**1549.9**, 1548.0	1131.0
II	1630.1, 1621.6	1163.9, 1156.4	1619.9, 1621.4	1613.3
	1597.5	1145.7	1597.3	1156.0, 1144.9
	1106.1	940.3	1085.7	1045
	685	533.6	675	600
	658.9		654.8	
III	1971.8	1857.5	1901.1	1970.2, 1856.1
	1691.2	1211.3	1691.4	1680, 1652.6
	1683, 1679	1205, 1202	1683, 1679	1645.8, 1204.6, 1222
	697	564	690	
			624	
	576.5		574.8	551.4

[a] All frequencies are in cm^{-1}. Stronger absorptions in split band are bold.

The observed product bands in this study, parallel to the case of Zr + ethylene, can be sorted into three groups on the basis of their behaviors upon photolysis and annealing and the results of calculations, where each group arises from a different reaction product. Group I absorptions grow on irradiation with λ > 530 nm; however, they remain almost the same in the following photolysis with λ > 290 nm and decrease on annealing. Group II absorptions increase most on photolysis with light, not only longer than 530 nm, but 290−320 nm as well. They are the only group of absorptions that grow on annealing up to 26 K. The absorptions of group III grow slightly on 290−320 nm irradiation, as well as λ > 530 nm, and they decrease on annealing. The observed frequencies of the product absorptions of the Hf + ethylene reaction are listed in three groups in Table 1. The Hf−H stretching absorptions are the strongest, and because of the heavy hafnium atom, the Hf−H stretching modes are effectively decoupled from other vibrational modes of the complexes. The hydrogen stretching absorption of group I (Figures 1 and 2) indicates that this reaction product probably

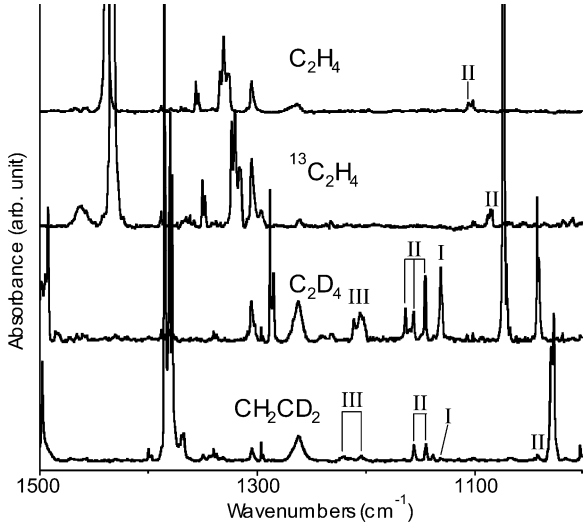

Figure 3. IR spectra in the region of 1000−1500 cm^{-1} for laser-ablated Hf atoms codeposited with ethylene isotopomers diluted in Ar at 7 K. I, II, or III indicates the absorption group.

contains a −HfH group, whereas the hydrogen stretching absorptions of groups II and III are 20 cm^{-1} or more apart, suggesting that these reaction products have $-HfH_2$ or $-HfH_3$ groups.

Several absorptions are assigned to group I as listed in Table 1. The split absorption at 1578.7 and 1576.8 cm^{-1}, the lowest Hf−H stretching frequency, is attributed to the mostly Hf−H stretching mode arising from two different sites in the matrix. The H/D ratio (1578.7/1163.9 = 1.356) and negligible C-13 shift are in agreement with this mode description. Our calculations predict the mostly C═C mode to be almost coincident, but with $^{13}C_2H_4$, the mostly C═C mode shifts to 1549.9 cm^{-1} and, with C_2D_4, to 1380.0 cm^{-1}, having the same band contour. Although the group I absorptions increase along with other product absorptions on photolysis (λ > 530 nm), they weaken most on annealing, as shown in Figure 1, indicating that they originate from a less stable reaction product, which eventually transforms thermally to more stable ones.

The increase of five group II absorptions on both irradiation and annealing indicates that the absorptions probably arise from a more stable reaction product. The absorption at 1597.5 cm^{-1} and the two absorptions at 1621.6 and 1630.1 cm^{-1} are attributed to the antisymmetric and symmetric stretching modes of an HfH_2 subunit. Figure 3 compares IR spectra in the 1000−1500 cm^{-1} region for Hf atoms codeposited with ethylene isotopomers diluted in Ar at 7 K. The absorption at 1106.1 cm^{-1} exhibits isotope shifts of −20.4 and −165.8 cm^{-1} by ^{13}C and D substitutions ($^{12}C/^{13}C$ and H/D isotopic ratios of 1.019 and 1.176). Most likely, the band arises from a CCH bending mode. Another band observed at 685 cm^{-1} in Figure 4 gives a small ^{13}C isotope shift of −10 cm^{-1} but a sizable D isotope shift of −151.4 cm^{-1}. The absorptions presumably originate from a predominantly HfH_2 valence angle bending mode.

Figure 5 shows a product absorption at 1971.8 cm^{-1} in the spectrum of Hf + C_2H_4, and similar absorptions are also found in the spectra of the isotopomers. The isotopic shifts on ^{13}C and D substitutions are −70.7 and −114.3 cm^{-1} ($^{12}C/^{13}C$ and H/D isotopic ratios of 1.037 and 1.062). On the basis of the frequencies and the large ^{13}C isotopic shift, the bands most probably arise from the C≡C stretching mode of a reaction product. Two counterparts are found with CH_2CD_2, at 1970.2 and 1856.1 cm^{-1}, just 1.6 and 1.4 cm^{-1} below the CH_2CH_2 and CD_2CD_2 values. The C≡C stretching absorption of polymeric acetylene is observed in this region,[28,29] but the C_2D_2 counterpart shifts to 1760 cm^{-1}, tracking C_2D_2 itself, which is far below the present 1857.5 cm^{-1} deuterium counterpart. Acetylene produced in the reaction of ethylene with the metal atoms can also form a π-complex with the metal atom; however, a considerably lower C≡C stretching frequency, due to the weakened C≡C bond, and a much weaker absorption are expected for the complex. The observed relatively strong absorption indicates that the C≡C triple bond is highly polarized by a substituent. Therefore, the absorptions probably arise from an ethynyl group bonded to a metal atom along the axis of the C≡C bond.

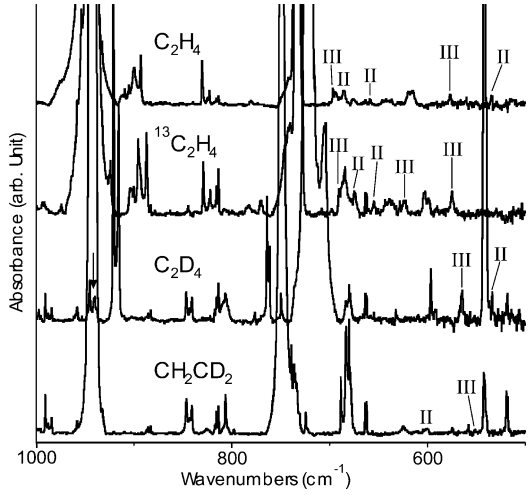

Figure 4. IR spectra in the region of 500−1000 cm^{-1} for laser-ablated Hf atoms codeposited with ethylene isotopomers diluted in Ar at 7 K. I, II, or III indicates the absorption group.

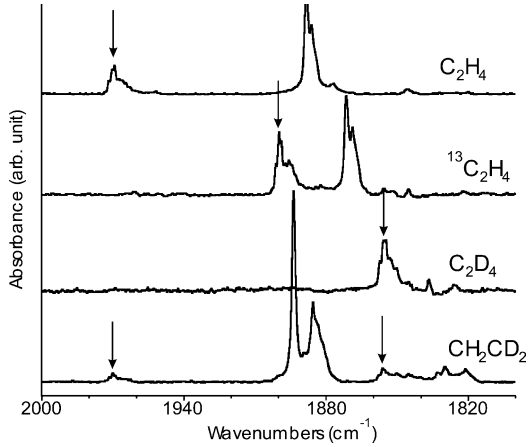

Figure 5. IR spectra in the C≡C stretching region. An arrow (↓) indicates the product absorption.

The strong Hf−H stretching absorptions of group III are observed at 1691.2, 1683, and 1679 cm^{-1}, with the latter two features overlapped (Figure 1). Like many other metal hydrides, the hydrogen stretching frequency of hafnium hydrides generally increases with the number of Hf−H valence bonds, and the Hf−H stretching band of HfH_4 is observed at 1683.2 cm^{-1}.[21,22] The Hf−H stretching frequencies of group III, much higher than those of groups I and II, suggest that the reaction product responsible to group III probably is a trihydrido C−H insertion complex, which, therefore, possesses a $-HfH_3$ group with the Hf atom bonded to an ethynyl group. The most probable energetically favorable product that fits the characteristics of the C≡C and Hf−H stretching absorptions is ethynyl hafnium trihydride (H−C≡C−Hf−H_3).

TABLE 2: Calculated Vibrational Characteristics of the Hafnium Metallacyclopropane Complex[a]

	C_2H_4		C_2D_4		$^{13}C_2H_4$		CH_2CD_2	
description	freq.	int.	freq.	int.	freq.	int.	freq.	int.
ν_1 A$_1$ CH_2 str.	3063.8	1	2230.1	2	3057.7	0	3060.3	3
ν_2 A$_1$ C═C str.	1419.2	1	1123.1	10	1412.3	0	1100.6	13
ν_3 A$_1$ CH_2 scis.	1031.8	28	884.5	8	1004.1	28	945.5	11
ν_4 A$_1$ CH_2 rock	835.1	4	638.8	10	826.9	3	705.1	7
ν_5 A$_1$ HfC_2 str.	449.7	8	425.5	6	435.7	8	427.0	8
ν_6 A$_2$ CH_2 str.	3115.2	0	2314.8	0	3103.2	0	2319.1	0
ν_7 A$_2$ CH_2 rock	1182.4	0	920.4	0	1171.5	0	1079.8	0
ν_8 A$_2$ CH_2 twist	364.6	0	265.8	0	363.0	0	290.5	0
ν_9 B$_1$ CH_2 str.	3132.7	2	2323.2	1	3120.7	2	3124.0	1
ν_{10} B$_1$ CH_2 rock	736.8	1	526.7	1	736.1	1	606.0	1
ν_{11} B$_1$ HfCH bend	478.5	0	352.2	0	476.8	0	438.9	0
ν_{12} B$_2$ CH_2 str.	3056.7	6	2212.4	2	3051.4	6	2221.3	2
ν_{13} B$_2$ CH_2 scis.	1403.9	2	1032.9	3	1399.4	2	1411.6	1
ν_{14} B$_2$ CH_2 wag	936.7	3	794.9	0	922.0	3	892.4	2
ν_{15} B$_2$ HfC_2 str.	497.9	18	429.4	15	484.7	17	470.0	15

[a] Frequencies (freq., unscaled) and intensities (int.) are in cm^{-1} and km/mol, respectively. Calculated at B3LYP/6-311+G(2d,p)/LANL2DZ level.

Assignments are made on the basis of the vibrational characteristics, behaviors on photolysis and annealing, the similarity to the vibrational characteristics in the Zr + ethlylene spectrum,[15] and calculated frequencies for anticipated products (Tables 2−5). The observed hydrogen stretching frequency for group I (1578.7 cm^{-1}) is more than 40 cm^{-1} lower than that of hafnium dihydride (1622.4 cm^{-1}).[21] Group I is attributed to the monohydrido C−H insertion complex (H−Hf−$CHCH_2$), and the assigned absorptions are listed in Table 3. Other than the Hf−H(D) stretch, which has also been observed for C_2D_4 and $C_2H_2D_2$ reaction products, the absorptions are computed to be very weak. However, the mostly C═C stretching mode is observed for H−Hf−$^{13}C_2H_3$ and D−Hf−C_2D_3, although this mode is coincident and masked by the Hf−H mode for H−Hf−C_2H_3.

On the other hand, the largest growth in intensity of group II absorptions on photolysis and annealing suggests that these absorptions originate from the most stable intermediate. Furthermore, the hydrogen stretching absorptions of group II are also observed in the hydrogen stretching region for hafnium dihydride. Group II absorptions are therefore assigned to the dihydrido C−H insertion complex (H_2−Hf−C_2H_2), which is the most stable reaction intermediate for the HfC_2H_4 stoichiometry (Table 6). Many group II absorptions are quite strong,

TABLE 3: Observed and Calculated Fundamental Frequencies of the Monohydrido C−H Insertion Complex of Hafnium and Ethylene Isotopomers[a]

										CH_2CD_2					
approximate mode	C_2H_4			C_2D_4			$^{13}C_2H_4$			H−Hf−CH CD_2			D−Hf−$CDCH_2$		
description	exptl	calcd	int.	exptl	calcd	int.	exptl	calcd	int.	exptl	calcd	int.	exptl	calcd	int.
ν_1 A′ CH str.		3176	2		2354	0		3166	2		3175	2		2347	1
ν_2 A′ CH_2 str.		3128	8		2307	3		3118	8		2313	2		3130	8
ν_3 A′ CH_2 str.		2868	35		2098	22		2860	35		2099	20		2868	36
ν_4 A′ HfH str.[b]	1579	1621	251	1132	1147	214	1578	1618	402	1578	1618	417	1131	1149	161
ν_5 A′ C═C str.[b]		1614	176	1380	1435	14	1550	1600	26		1447	23		1615	9
ν_6 A′ CH_2 scis.[b]	*c*	1386	43	*c*	1095	20	*c*	1346	40		1095	27		1373	38
ν_7 A′ CH_2 scis.		1223	17		1012	8		1205	18		1154	14		1139	60
ν_8 A′ CH_2 rock		897	13		650	8		895	13		777	9		734	8
ν_9 A′ CHf str.		589	18		518	10		575	18		551	18		537	10
ν_{10} A′ CHfH IP bend		379	28		291	8		375	28		377	28		298	6
ν_{11} A′ CCHf IP bend		251	28		217	26		245	26		230	23		233	30
ν_{12} A″ CH_2 twist		988	7		757	1		982	7		924	16		888	7
ν_{13} A″ CH_2 wag		862	29		668	19		854	28		691	15		795	19
ν_{14} A″ CCHf OOP bend		419	21		308	11		418	21		343	19		374	15
ν_{15} A″ CHfH OOP bend		175	5		129	2		174	5		161	4		136	2

[a] Frequencies and intensities are in cm^{-1} and km/mol, respectively. Intensities are all calculated values. Calculated at B3LYP/6-311+G(2d,p)/LANL2DZ level. [b] Mixed modes. [c] Possible absorption masked by acetylene product absorptions.

TABLE 4: Observed and Calculated Fundamental Frequencies of the Dihydrido Complexes of Hafnium and Ethylene Isotopomers[a]

	$HfH_2-C_2H_2$			$HfD_2-C_2D_2$			$HfH_2-^{13}C_2H_2$			HfHD−C_2HD		
description	exptl	calcd	int.	exptl	calcd	int.	exptl	calcd	int.	exptl	calcd	int.
ν_1 A′ CH str. (s)		3159	4		2353	0		3147	5		2336	2
ν_2 A′ CH str. (a)		3129	8		2304	2		3120	9		3135	7
ν_3 A′ HfH_2 s. str.	1630	1653	308	1164	1169	160	1630	1652	310	1613	1629	401
ν_4 A′ CC str.		1414	8		1372	1		1362	7		1392	5
ν_5 A′ CCH IP a. bend	1106	1134	64	940	957	23	1086	1117	66	1045	1074	50
ν_6 A′ CCH IP s. bend		855	7		613	2		854	7		722	12
ν_7 A′ HfH_2 scis.	685	687	153	534	578	80	675	683	148	600	627	122
ν_8 A′ HfC_2 a. str.		616	78		538	71		599	74		556	69
ν_9 A′ HfC_2 s. str.		550	4		448	16		535	6		530	2
ν_{10} A′ HfH_2 wag		187	315		134	161		187	315		154	205
ν_{11} A″ HfH_2 a. str.	1598	1605	517	1146	1142	264	1597	1606	517	1156	1156	223
ν_{12} A″ CCH a.OOP		976	0		772	0		967	0		901	10
ν_{13} A″ CCH s.OOP	659	662	70		504	39	655	658	69		555	44
ν_{14} A″ HfH_2 rock		386	1		279	2		385	1		309	5
ν_{15} A″ HfH_2 twist		356	12		272	4		353	13		326	38

[a] Frequencies (unscaled) and intensities are in cm^{-1} and km/mol, respectively. Intensities are all calculated values. Calculation at B3LYP/6-311+G(2d,p)/LANL2DZ level.

TABLE 5: Observed and Calculated Fundamental Frequencies of the Trihydrido C−H Insertion Complex of Hafnium and Ethylene (Ethynyl Hafnium Trihydride)[a]

										CH_2CD_2					
	H_3−Hf−CCH			D_3−Hf−CCD			H_3−Hf−$^{13}C^{13}$CH			H_2D−Hf−CCD			HD_2−Hf−CCH		
description	exptl	calcd	int.	exptl	calcd	int.	exptl	calcd	int.	exptl	calcd	int.	exptl	calcd	int.
ν_1 A_1 C−H str.		3432	29		2655	0		3414	32		2655	0		3432	29
ν_2 A_1 CC str.	1972	2067	145	1858	1933	161	1901	2000	128	1856	1933	149	1970	2067	151
ν_3 A_1 HfH_3 s. str.	1691	1768	237	1211	1252	117	1691	1768	240	1680	1750	306	1653	1732	365
ν_4 A_1 HfH_3 s. def.	577	606	256		463	184	575	605	251		551	208	551	563	111
ν_5 A_1 C−Hf str.		426	32		389	2		413	32		417	29		411	10
ν_6 E HfH_3 a. str.	1683	1714	899	1205	1217	461	1683	1714	899	1646	1714	444	1222	1240	163
										1205	1229	207		1218	237
ν_7 E CCH bend	697	717	75	564	570	29	690	709	76		570	10		717	37
											568	2		717	37
ν_8 E HfH_3 a. def.		658	102		467	44	624	658	104		645	93		573	60
											580	26		468	117
ν_9 E HfH_3 rock		387	155		297	104		385	150		361	79		319	61
											322	48		312	49
ν_{10} E CCHf bend		167	7		146	3		163	7		155	3		162	2
											150	2		156	2

[a] Frequencies (unscaled) and intensities are in cm^{-1} and km/mol, respectively. Intensities are all calculated values. Calculation at B3LYP/6-311+G(2d,p)/LANL2DZ level.

TABLE 6: Geometrical Parameters and Physical Constants of the Mono-, Di-, Trihydrido C−H Insertion Products in Reaction of Ethylene with Laser-Ablated Hf Atoms[a]

parameters	Hf−C_2H_4	H−Hf−$CHCH_2$	H_2−Hf−C_2H_2	H_3−Hf−CCH
r(C−C)	1.495	1.346	1.348	1.215
r(C−H)	1.089	1.084, 1.087, 1.110	1.085, 1.087	1.066
r(C−Hf)	2.152	2.119, 2.519	2.077, 2.103	2.152
r(Hf−H)		1.862	1.862	1.824
∠CCH	117.8	120.4, 122.2, 127.4	127.3, 130.1	180.0
∠HCH	111.5	110.4		
∠CHfC	40.7	32.3	37.6	0.0
∠CHfH		128.9	108.5, 118.9	110.8
∠HHfH			120.6	108.1
∠HCHf		149.2	157.7, 162.6	110.8
Φ(HCCHf)	110.8	0.0	180.0	
Φ(HCHfH)		0.0	66.4, 97.0	
Φ(HCCH)	138.5	180.0	0.0	
Φ(CCHfH)		180.0	83.0, 113.6	
mol. symm.	C_{2v}	C_s	C_s	C_{3v}
q(C)[b,c]	−0.38	−0.76, 0.18	−0.39, −0.34	−0.83, −0.31
q(H)[b,c]	0.11	−0.20, 0.08, 0.08, 0.10	−0.23, −0.23, 0.07, 0.08	−0.25, −0.25, −0.25, 0.16
q(Hf)[b]	0.32	0.53	1.05	1.71
μ[d]	1.19	2.36	1.94	1.43
$^1\Delta E$[e]	49.35 ($^1A_1$)	35.06 (^1A)	64.64 ($^1A'$)	60.25 ($^1A_1$)
$^3\Delta E$[e]	32.39 ($^3B_1$)	40.69 ($^3A''$)	27.02 (^3A)	f

[a] Bond lengths and angles are in Å and deg. Calculated at B3LYP/6-311+G(2d,p)/LANL2DZ level. [b] Mulliken atomic charge. [c] Numbers are in the order from the closest one to the metal atom to the farthest. [d] Molecular dipole moment in D. [e] Binding energies in kcal/mol in the singlet and triplet ground electronic states. [f] Attempt to find an optimized geometry converged to the triplet dihydrido complex.

and the observed characteristics of group II absorptions summarized in Table 4 show very good agreement with the calculated values. The five calculated frequencies are 0.3−1.4% higher than observed values, which is comparable to previous B3LYP calculaions for first-row transition-metal inorganic molecules.[30]

The mono- and dihydrido C−H insertion complexes (H−Hf−$CHCH_2$ and H_2−Hf−C_2H_2) are, in fact, reaction intermediates presumed in reaction dynamics studies of hydrogen elimination of ethylene by vaporized early second-row transition-metal atoms.[11,12] This strongly suggests that hydrogen elimination also readily occurs by early third-row transition-metal atoms. The Hf + ethylene reaction most likely has a similar potential energy surface along the reaction coordinates to that of the Zr + ethylene reaction, because the mono- and dihydrido C−H insertion complexes are also produced in the reaction of ethylene with laser-ablated Zr atoms,[15] as also predicted in theoretical investigations.[11]

Group III is attributed to the trihydrido C−H insertion complex (H_3−Hf−CCH, ethynyl hafnium trihydride). The absorptions in the C≡C stretching region at 1972 cm^{-1}, and the strong symmetric Hf−H stretching absorptions at 1691 cm^{-1} and antisymmetric (degenerate) Hf−H stretching mode split at 1683 and 1679 cm^{-1} suggest that an acetylene group is bonded to a metal atom along the C≡C bond axis, while three hydrogen atoms are bonded to the metal atom as described already. The observed vibrational characteristics of group III are compared with the calculated values in Table 5, showing satisfactory agreements between the observed and calculated values. The calculated frequencies are 1.8−5.0% higher than observed for this challenging subject molecule. This also includes the anticipated red argon matrix shift. Considerable effort was undertaken to find other states and structures to improve the frequency fit, but none were found. However, it is worthwhile to point out that the energy of the singlet trihydrido complex is comparable to that of the dihydrido complex as shown in Table 6. Further attempts to optimize the geometry of the trihydrido complex in the lowest triplet state end up with the structure of the dihydrido complex in a higher-energy triplet state. The two complexes are probably easily interconvertible in the lowest triplet state during the reaction of ethylene and hafnium atoms, and it is also notable that the reaction of ethylene with the vaporized Hf atom ($^3F_2$) most probably starts on the triplet potential surface.

Calculations have been carried out at the B3LYP/6-311+G(2d,p)/LANL2DZ level for the metallacyclopropane (Hf−C_2H_4), the mono-, di-, and trihydrido C−H insertion products (H−Hf−$CHCH_2$, H_2−Hf−C_2H_2, and H_3−Hf−CCH), and other related compounds. The geometrical parameters and molecular constants of the metallacyclopropane and the three C−H insertion products are summarized in Table 6, and the optimized molecular structures and ground states are shown in Figure 6. The calculated frequencies for possible product molecules are listed along with the experimental values in Tables 2−5.

The calculations show that a singlet state ($^1A_1$) is the ground state for the metallacyclopropane complex, while a triplet state

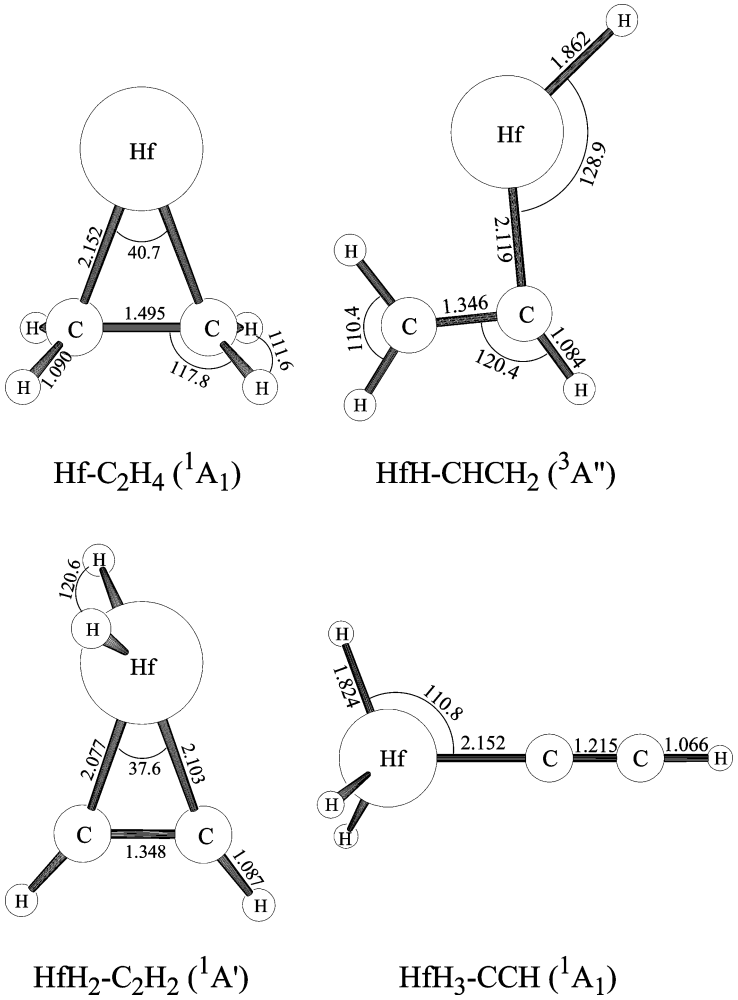

Figure 6. The optimized molecular structures (B3LYP/6-311+G(2d,p)/LANL2DZ) of the reaction intermediates in their ground electronic states. The bond lengths and angles are in Å and deg, respectively, and the electronic states are shown in parentheses.

($^3A''$) is lowest for the monohydrido C−H insertion complex. The monohydride is fully relaxed with no symmetry: When constricted to planar, the energy and frequencies are essentially unchanged but some intensities are altered. On the other hand, singlet ground states are favored for compounds with more Hf bonds, and singlet ground states are found for the di- and trihydrido complexes. It is generally accepted that, along the reaction path of hydrogen elimination by second-row transition-metal atoms, the energy barrier to CH activation for formation of the monohydrido C−H insertion complex is the highest one, and no barriers lie above the reactant asymptote all the way to H_2 elemination.[11]

The insertion complex has a planar structure at its triplet ground state. Although the length of the Hf−C bond is slightly shorter than those of metallacyclopropane complex, the length of the C−C bond (1.34 Å) is close to that of a C=C double bond. The C−H insertion from the metallacyclopropane also leads to a large increase in infrared absorption. Particularly, the Hf−H stretching absorptions of the insertion products are dramatically stronger than those of the metallacyclopropane, as shown in Tables 2−5.

The dihydrido C−H insertion complex has a C_S structure in its singlet ground state as illustrated in Figure 6. The Hf−H and C−C bond lengths are similar to those of H−Hf−C_2H_3 insertion complex. Calculations indicate that the dihydrido complex is the most stable among the Hf−ethylene complexes considered here, which is consistent with the stability of the dihydrido complex observed on annealing and photolysis. Previous reaction dynamics studies assume that the detachment of hydrogen occurs from the dihydrido complex in the hydrogen elimination reaction.[6−13]

The measured metal−hydrogen stretching frequencies and the M−H and C−M bond lengths of the C−H insertion complexes of ethylene with Ti, Zr, and Hf atoms in the ground electronic states are listed in Table 7. The hydrogen stretching frequencies of Hf complexes are much higher than those of Zr complexes, and also higher than those of the Ti complexes. Moreover, the Hf−H and C−Hf bond lengths are shorter than the Zr−H and C−Zr bond lengths, respectively. The higher stretching frequencies and shorter bond lengths of the C−HfH_x insertion complexes are attributed to the larger relativistic bond-length contraction for Hf as predicted by Pyykko et al.[16−19]

As in the reaction of ethylene with laser-ablated zirconium atoms,[15] acetylene is produced in large extent. We estimate that 20% of ethylene is converted to acetylene on the basis of the intensities of the hydrogen stretching absorptions of acetylene and ethylene in the region of 2800−3400 cm^{-1}. Although much of the acetylene is probably generated by vacuum UV light emitted from the target plume during laser ablation, the presence of the reaction intermediates of the hydrogen elimination of ethylene suggests that part of the acetylene originates from the hydrogen elimination of ethylene by the metal atom reactions.

Like previous matrix isolation studies on the reaction of ethylene with transition-metal atoms,[14,15,31] no absorption from the Hf metallacyclopropane complex has been identified, probably because the vibrational bands are mostly very weak

TABLE 7: M−H Stretching Frequencies and Bond Lengths of Mono-, Di-, and Trihydrido C−H Insertion Complexes ($H-M-CHCH_2$, $H_2-M-C_2H_2$, and $H_3-M-CCH$) in the Ground Electronic States[a]

	$H-M-CHCH_2$	$H_2-M-C_2H_2$	$H_3-M-CCH$	description
Ti[b]	1500.0	1610.5, 1585.0	*c*	Ti−H str.
	1080.4	1157.5, 1151.9	*c*	Ti-D str.
	1.763	1.708	*c*	*r*(Ti−H)
	2.038	1.947, 1.976	*c*	*r*(C−Ti)
Zr[d]	1519.8	1567.3, 1536.9	1638.6, 1628.8, 1620.8	Zr−H str.
	1094.6	1120.1, 1114.6	1177.7, 1171.0, 1164.8	Zr-D str.
	1.879	1.869	1.838	*r*(Zr−H)
	2.161	2.103, 2.133	2.176	*r*(C−Zr)
Hf	1578.7	1630.1, 1597.5	1691.2, 1683, 1679	Hf−H str.
	1131.6	1163.9, 1145.7	1211.3, 1205, 1202	Hf-D str.
	1.862	1.862	1.824	*r*(Hf−H)
	2.119	2.077, 2.103	2.152	*r*(C−Hf)

[a] Frequencies are all measured values in cm^{-1}, whereas bond lengths are calculated values in Å. [b] Ref 14. Experiments performed with laser-ablated Ti and C_2H_4 produce the same major products; ref 30. [c] Trihydrido C−H insertion complexes are not identified; refs 14, 30. [d] Ref 15.

as shown in Table 2. As a result, conversion from a possible metallacyclopropane complex to the mono-, di-, and trihydrido insertion products should increase the intensities of the corresponding absorptions without noticeable decrease in intensities of any absorptions in the spectrum as observed.

Conclusions

Consistent with the case of Zr + ethylene,[15] the mono-, di-, and trihydrido C−H insertion Hf−ethylene complexes are produced in the reaction of ethylene with laser-ablated Hf atoms and identified in a solid argon matrix. The mono- and dihydrido complexes are intermediates in the H_2 elimination reaction of ethylene by second-row transition-metal atoms presumed in previous reaction dynamics studies.[11] The previous and present results show that the reaction of laser-ablated transition-metal atoms with hydrocarbons is a prominent method to produce novel C−H insertion products, which may play important roles as intermediates in the hydrogen elimination reactions. Evidence of lanthanide contraction by relativistic effects on electrons is also found: The Hf−H stretching frequencies of the insertion products are higher than the corresponding Ti−H and Zr−H frequencies, and the Hf−H and C−Hf bonds are shorter than the Zr−H and C−Zr bonds, respectively.

Acknowledgment. We gratefully acknowledge financial support for this work from N.S.F. Grant CHE 00-78836 and sabbatical leave support (H.-G. Cho) from the Korea Research Foundation (KRF-2003-013-C00044).

References and Notes

(1) Siegbahn, P. E. M.; Blomberg, M. R. A.; Svensson, M. *J. Am. Chem. Soc*. **1993**, *115*, 1952.

(2) Blomberg, M. R. A.; Siegbahn, P. E. M.; Svensson, M. *J. Phys. Chem*. **1992**, *96*, 9794.

(3) Yi, S. S.; Blomberg, M. R. A.; Siegbahn, P. E. M.; Weisshaar, J. C. *J. Phys. Chem. A* **1998**, 102.

(4) Blomberg, M. R. A.; Siegbahn, P. E. M.; Yi, S. S.; Noll, R. J.; Weisshaar, J. C. *J. Phys. Chem. A* **1999**, *103*, 7254.

(5) Parnis, J. M. P.; Lafleur, R. D.; Rayner, D. M. *J. Phys. Chem*. **1995**, *99*, 673.

(6) Carroll, J. J.; Haug, K. L.; Weisshaar, J. C.; Blomberg, M. R. A.; Siegbahn, P. E. M.; Svensson, M. *J. Phys. Chem*. **1995**, *99*, 13955.

(7) Reichert, E. L.; Yi, S. S.; Weisshaar, J. C. *Int. J. Mass Spectrom*. **2000**, *196*, 55.

(8) Wen, Y.; Poremski, M.; Ferrett, T. A.; Weisshaar, J. C. *J. Phys. Chem. A* **1998**, *102*, 8362.

(9) Poremski, M.; Weisshaar, J. C. *J. Phys. Chem*. *A* **2000**, *104*, 1524.

(10) Carroll, J. J.; Haug, K. L.; Weisshaar, J. C. *J Am. Chem. Soc*. **1993**, *115*, 6962.

(11) Poremski, M.; Weissharr, J. C. *J. Phys. Chem. A* **2001**, *105*, 4851.

(12) Willis, P. A.; Stauffer, H. U.; Hinrichs, R. Z.; Davis, H. F. *J. Phys. Chem. A* **1999**, *103*, 3706.

(13) Stauffer, H. U.; Hinrichs, R. Z.; Schroden, J. J.; Davis, H. F. *J. Phys. Chem. A* **2000**, *104*, 1107.

(14) Lee, Y. K.; Manceron, L.; Papai, I. *J. Phys. Chem. A* **1997**, *101*, 9650.

(15) Cho, H.-G.; Andrews, L. *J. Phys. Chem. A* **2004**, *108*, 3965.

(16) Pyykko, P.; Desclaux, J. P. *Chem. Phys. Lett*. **1977**, *50*, 503.

(17) Pyykko, P.; Snijders, J. G.; Baerends, E. J. *Chem. Phys. Lett*. **1981**, *83*, 432.

(18) Ziegler, T.; Snijders, J. G.; Baerends, E. J. *J. Chem. Phys*. **1981**, *74*, 1271.

(19) Pyykko, P. *Chem. Rev*. **1988**, *88*, 563.

(20) Chertihin, G. V.; Andrews, L. *J. Am. Chem. Soc*. **1995**, *117*, 6402.

(21) Chertihin, G. V.; Andrews, L. *J. Phys. Chem*. **1995**, *99*, 15004.

(22) Cho, H.-G.; Andrews, L. *Organometallics* **2004**, *23*, 4357.

(23) Burkholder, T. R.; Andrews, L. *J. Chem. Phys*. **1991**, *95*, 8697.

(24) Hassanzadeh, P.; Andrews, L. *J. Phys. Chem*. **1992**, *96*, 9177.

(25) Andrews, L.; Zhou, M.; Chertihin, G. V.; Bauschlicher, C. W., Jr. *J. Phys. Chem. A* **1999**, *103*, 6525.

(26) Zhou, M F.; Andrews, L.; Bauschlicher, C. W., Jr. *Chem. Rev*. **2001**, *101*, 1931.

(27) Frisch, M. J.; Trucks, G. W.; Schlegel, H. B.; Scuseria, G. E.; Robb, M. A.; Cheeseman, J. R.; Zakrzewski, V. G.; Montgomery, J. A., Jr.; Stratmann, R. E.; Burant, J. C.; Dapprich, S.; Millam, J. M.; Daniels, A. D.; Kudin, K. N.; Strain, M. C.; Farkas, O.; Tomasi, J.; Barone, V.; Cossi, M.; Cammi, R.; Mennucci, B.; Pomelli, C.; Adamo, C.; Clifford, S.; Ochterski, J.; Petersson, G. A.; Ayala, P. Y.; Cui, Q.; Morokuma, K.; Rega, N.; Salvador, P.; Dannenberg, J. J.; Malick, D. K.; Rabuck, A. D.; Raghavachari, K.; Foresman, J. B.; Cioslowski, J.; Ortiz, J. V.; Baboul, A. G.; Stefanov, B. B.; Liu, G.; Liashenko, A.; Piskorz, P.; Komaromi, I.; Gomperts, R.; Martin, R. L.; Fox, D. J.; Keith, T.; Al-Laham, M. A.; Peng, C. Y.; Nanayakkara, A.; Challacombe, M.; Gill, P. M. W.; Johnson, B.; Chen, W.; Wong, M. W.; Andres, J. L.; Gonzalez, C.; Head-Gordon, M.; Replogle, E. S.; Pople, J. A. *Gaussian 98*, Revision A.11.4; Gaussian, Inc.: Pittsburgh, PA, 2002.

(28) Wang, X.; Andrews, L. *J. Phys. Chem. A* **2004**, *108*, 4838 (Pt + C_2H_2).

(29) Andrews, L.; Kushto, G. P.; Marsden, C. To be published (U, Th + C_2H_2).

(30) Bytheway, I.; Wong, M. W. *Chem. Phys. Lett.* **1998**, *282*, 219.

(31) Cho, H.-G.; Andrews, L. Unpublished (Ti + C_2H_4).